Tissue engineered bone: Measurement of nutrient transport in three-dimensional matrices

Edward A. Botchwey,[1–4] Melissa A. Dupree,[3] Solomon R. Pollack,[3] Elliot M. Levine,[4] Cato T. Laurencin[1,2,5]
[1]*Department of Biomedical Engineering, The University of Virginia, 400 Ray C. Hunt Drive, Suite 330, Charlottesville, Virginia 22903*
[2]*Department of Orthopaedic Surgery, The University of Virginia, Charlottesville, Virginia 22903*
[3]*Department of Bioengineering, University of Pennsylvania, Philadelphia, Pennsylvania*
[4]*The Wistar Institute, Philadelphia, Pennsylvania*
[5]*Department of Chemical Engineering, The University of Virginia, Charlottesville, Virginia 22903*

Received 28 October 2002; revised 3 March 2003; accepted 21 March 2003

Abstract: The classic paradigm for *in vitro* tissue engineering of bone involves the isolation and culture of donor osteoblasts or osteoprogenitor cells within three-dimensional (3D) scaffold biomaterials under conditions that support tissue growth and mineralized osteoid formation. Our studies focus on the development and utilization of new dynamic culture technologies to provide adequate nutrient flux within 3D scaffolds to support ongoing tissue formation. In this study, we have developed a basic one-dimensional (1D) model to characterize the efficiency of passive nutrient diffusion and transport flux to bone cells within 3D scaffolds under static and dynamic culture conditions. Internal fluid perfusion within modeled scaffolds increased rapidly with increasing pore volume and pore diameter to a maximum of approximately 1% of external fluid flow. In contrast, internal perfusion decreased significantly with increasing pore channel tortuosity. Calculations of associated nutrient flux indicate that static 3D culture and some inappropriately designed dynamic culture environments lead to regions of insufficient nutrient concentration to maintain cell viability, and can result in steep nutrient concentration gradients within the modeled constructs. These quantitative studies provide a basis for development of new dynamic culture methodologies to overcome the limitations of passive nutrient diffusion in 3D cell-scaffold composite systems proposed for *in vitro* tissue engineering of bone. © 2003 Wiley Periodicals, Inc. J Biomed Mater Res 67A: 357–367, 2003

Key words: tissue engineering; scaffold; bone; diffusion; flow

NOMENCLATURE

V_∞ Velocity of scaffold motion relative to the fluid of the rotating bioreactor (m s^{-1})

V Calculated fluid perfusion velocity through the scaffold (m s^{-1})

∇P Pressure gradient across the scaffolds is approximated by average pressure difference, ΔP, per unit length.[24]

$$\nabla P \approx \frac{\Delta P}{L} \text{ (N m}^{-1}\text{)}$$

Correspondence to: C. T. Laurencin; e-mail: ctl3f@virginia.edu

Contract grant sponsor: NASA; contract grant number: NAG9-832
Contract grant sponsor: NIH; contract grant number: AR07132-23
Contract grant sponsor: NSF; contract grant number: 0115404

K Darcy's permeability constant (m^2)

ϵ Fluid-filled volume fraction

δ Median pore diameter of the scaffold (m)

τ Tortuosity (pore path length per unit scaffold thickness). Estimated microcarrier scaffold tortuosity of 2.5 was accepted by the authors for modeling of glucose flux

σ Cross-sectional area of an individual pore (m^2)

N Total number of cells within the scaffold

n Total number of cylindrical pores

R Length of the scaffold (m)

L Thickness of the scaffold (m)

l Length of the cylindrical pores within the scaffold (m)

D Diffusivity of glucose[26]

$$D = 6.6 \times 10^{-10} \text{ m}^2 \text{ s}^{-1}$$

$\hat{r}$ Single osteoblast rate of glucose consumption[33]

$$\hat{r} = 1.6 \times 10^{-14} \text{ g s}^{-1}$$

η Dynamic viscosity of water at 30°C[34]

$$\eta = 0.799 \times 10^{-3}\ \text{kg m}^{-1}\ \text{s}^{-1}$$

Δx Incremental depth within modeled microcarrier scaffolds (m)

ΔM Fluid-filled pore volume at depth Δx within modeled scaffolds (m^3)

ΔQ Quantity of glucose delivered within volume ΔM under model fluid flow conditions (g)

T Average residence time of fluid perfusing through depth Δx within model microcarrier scaffolds (s)

INTRODUCTION

Surgical repair of bony defects has become an increasingly significant problem in orthopedic medicine.[1] Autogenous bone graft, or autograft, derived from the iliac crest has long been considered the "gold standard" biological graft material used most frequently and successfully for skeletal reconstruction, but despite its success, supply limitations and concerns over postoperative morbidity fuel a growing desire for clinically viable alternatives.[2] From 1997 to 1999 alone, the market for bone grafts and bone substitutes has grown by more than 40% to a 270 million dollar (+) industry.[1] Currently, clinical alternatives to autografts include allogenic bone, ceramics, demineralized bone matrix, bone marrow, and composite grafts (consisting of combinations of materials), but none of these materials has been met with widespread acceptance.[1] As a result, much research interest has been directed toward the development of new tissue engineering strategies for bony repair.

The classic paradigm for *in vitro* tissue engineering of bone involves the isolation and culture of donor osteoblasts or osteoprogenitor cells within three-dimensional (3D) scaffold biomaterials under conditions that support tissue growth and mineralized osteoid formation.[1,3–11] By combining appropriately engineered biomaterials, culture conditions, and cells, strategies may ultimately be found to produce synthetic bone grafts capable of providing both initial mechanical support and the necessary osteoconductive/inductive and angiogenic interactions at the site of bony repair. To this end, a variety of porous, 3D scaffold systems based on a variety of ceramic and or degradable polymeric biomaterials have been proposed for osteoblastic cell cultivation and tissue engineering of bone.[10,12–15] However, one major constraint in the use of 3D scaffolds has been the limitation of cell migration and tissue ingrowth within these structures. Because cells located in the interior scaffold receive nutrients only through diffusion from the surrounding media in static culture, many investigators have speculated that high cell density on the exterior of the scaffold may deplete nutrient supply before these nutrients can diffuse to the scaffold interior to support tissue growth. In addition, diffusive limitations may also inhibit the efflux of cytotoxic degradation products from the scaffold and metabolic wastes produced in the scaffold interior. Over the years, ingrowth limitations have been observed for cell–scaffold composite systems proposed for tissue engineering of bone.[5,6,15–17] Select examples of possible diffusive limitations of high cell density 3D culture are summarized in Table I. In a series of related studies, maximum penetration depths of osseous tissues were reported[5,6] in the range of 200–300 μm within particulate leached poly(D,L-lactic-*co*-glycolic acid) (PLAGA) 3D foams after 56 days of static *in vitro* culture. In studies of osteoblastic cell growth on 3D constructs, our work and that of others have shown preferential short-term

TABLE I
Representative Examples of High-Density Bone Cell Cultivation Within 3-D Scaffolds

Cell Type	Pore Size (mm)	Pore Volume (%)	Scaffold Thickness (mm)	Cell Density (cells/mL)	Observation	Reference
Rat marrow	300–500	90	1.9	[a]	Maximum osseous penetration of 240 ± 82 μm (day 56)	Ishaug et al.[6]
Rat calvaria	150–300	90	1.9	[a]	Maximum osseous penetration of 220 ± 40 μm (day 56)	Ishaug-Riley et al.[5]
	500–710	90	1.9	[a]	Maximum osseous penetration of 190 ± 40 μm at (day 56)	
SaOS-2	187	30	2.5	9.5×10^7	Preferrential cell growth on scaffold exterior (day 7)	Botchwey et al.[19]
Rat marrow	300–500[b]	78	6	[b]5.8×10^6 [c]	Preferrential cell growth on scaffold exterior (day 7)	Goldstein et al.[17]

Note: Only data from Botchwey et al.[19] and Goldstein et al.[17] have been used for modeling of glucose diffusion.
[a]Values of cell density within the scaffold could not be determined from the reference.
[b]An average pore diameter of 400 mm was assumed to facilitate model calculations.
[c]Reported values for cell and scaffold void volume of 3.5×10^6 and 0.60 cm^2 were used to determine cell density (cells/mL).

growth of osteoblastic cells on exterior regions of scaffolds exposed directly to surrounding culture medium.[16–19] Although several attempts in other systems have been made to alter scaffold geometry to provide adequate diffusion within 3D constructs with some success,[20,21] ingrowth limitations within 3D scaffolds remain a pervasive problem in tissue engineering.

To circumvent possible nutrient transport limitations in static 3D culture, various "dynamic" culture methods have been proposed to provide a well-mixed environment and possible culture medium flow within and around 3D scaffolds during cultivation.[16,17,19] Several dynamic culture systems have been proposed for tissue engineering of bone, including spinner flasks, rotating bioreactors, and direct perfusion cultures; however, there is no consensus on what specific dynamic culture conditions are most conducive to bone tissue synthesis and what technology is best suited to achieve those conditions. In a recent study, Shea et al.[16] examined osseous tissue ingrowth within particulate leached PLAGA scaffolds during long-term cultivation in a spinner flask bioreactor, and observed a precipitous decrease in cell density in interior regions of the scaffold possibly due to cell death. Goldstein et al.[17] went on to compare cell ingrowth within similarly designed scaffolds using several representative systems of dynamic culture, and showed that whereas cell ingrowth within spinner flasks resulted in decreases in interior cell density as previously reported, cultivation in rotating bioreactors and perfusion cultures yielded a more uniform distribution of cell growth throughout the scaffolds. However, a multiplicity of factors are present that may impact nutrient delivery and tissue synthesis in dynamic culture. These include a broad range of scaffold materials and designs, scaffold porosity and size, cell types, initial cell plating densities and methods, and experimental fluid flow conditions that result in nutrient transport during dynamic tissue engineering of bone. In this report, we will expand the quantitative basis for dynamic culture systems to supply adequate nutrient flux within 3D constructs to support ongoing tissue formation.

Previously, we described a new system of dynamic culture based on porous, lighter-than-water PLAGA scaffolds in the high aspect ration vessel rotating bioreactor,[19] and the development of quantitative methods to control the motion of these scaffolds through the culture medium of the bioreactor during rotating culture. The motion of the scaffolds facilitates culture medium flow to cells within the porous 3D network of the scaffolds. Preliminary studies of osteoblast-like cell cultivation in this system showed significant increases in alkaline phosphatase expression and mineralized osteoid synthesis *in vitro*. In this study, we have extended our analysis to quantitatively examine the role of nutrient delivery in our culture system and other 3D systems of high cell density. The objectives of this analytical and experimental study were twofold: 1. to characterize the efficiency of passive nutrient diffusion to bone cells within our 3D scaffolds under static culture conditions; and 2. to quantify the effects of internal fluid perfusion and flow-induced nutrient transport to cells within the scaffolds during dynamic bioreactor cultivation.

MATERIALS AND METHODS

Scaffold fabrication and characterization

Porous, lighter-than-water scaffolds of degradable PLAGA were prepared using sintered microsphere methods reported previously.[19] Briefly, spherical PLAGA microcarriers in the size range of 500–860 μm were poured into a stainless steel mold and thermally sintered for 1–5 h at 70°C. Scaffolds were fabricated in a range of predetermined densities to control the velocity and trajectory of the scaffold motion in the rotating bioreactor. The densities of the scaffold were modified by sintering both solid, heavier-than-water and hollow microcarriers in appropriate ratios within the same scaffold. The ratio of solid, heavier-than-water microcarriers and hollow, lighter-than-water microcapsules is given by mixing ratio, ϕ, which is defined as the mass ratio of solid microcarriers to that of hollow microcarriers within each scaffold. The scaffold densities were from approximately 0.99 ($\phi = 1$) to 0.65 g/mL ($\phi = 0$), resulting in measured scaffold velocities, relative to the culture medium, of between 3 to 100 mm/s. Relative motion of the scaffold in the rotating bioreactor was characterized by *in situ* imaging analysis. The measurement of physical scaffold properties and characteristic motion in the rotating bioreactor has been described previously in detail.[19] Briefly, scaffold pore volume, median pore size, and density were measured by mercury porosimetry (Autopore III porosimeter; Micromeritics, Norcross, GA). Scaffolds were fabricated in the shape of porous cylinders 4 mm in diameter and approximately 2.5 mm in length each having approximately 30% pore volume and 200-μm median pore size.

Exploratory evaluation of cell growth within the microcarrier scaffolds was done by light microscopic examination after scaffold bisection.[18] Briefly, select scaffolds, exhibiting the highest velocity in the bioreactor, were seeded with Saos-2 human osteoblast-like cells (ATCC no. HTB-85) and cultured under both static and dynamic conditions as described by Botchwey et al.[19] After 7 days of cultivation, scaffolds were removed and cells were stained for alkaline phosphatase using standard histochemical methods.[22] After cell staining, scaffolds were sectioned using a surgical blade along their central axis perpendicular to the front face of the disk. Cell growth and penetration within the scaffolds were assessed qualitatively by light microscopy.

Characterization of internal fluid flow

To quantify nutrition flux during dynamic culture within 3D scaffolds, it is necessary to create a suitable analytical

representation of these systems to facilitate our analysis. We have made the following simplifying assumptions, as has been described previously by Botchwey et al.[18]:

1. The scaffolds are roughly cylindrical and their 3D geometry may be represented by a network of interconnecting cylindrical channels with tortuosity, τ. The Darcy permeability constant, K, for such a construct has been described by Scheidegger[23] and is given by:

$$K = \frac{\varepsilon\sigma^2}{96\eta\tau^2}, \tag{1}$$

where ϵ is the pore volume fraction, σ is pore diameter, and η is the viscosity of the fluid. During the short but important time period of experimental validation used in this study, the physical dimensions and 3D geometry of the scaffold do not change. Over longer periods of time, the scaffold will degrade, thereby requiring an extension of the theoretical approach.

2. There is a homogeneous velocity profile, V_∞, at a large distance from the porous scaffold that creates a pressure gradient, ∇P, across the thickness of the construct.
3. The normal vector of the scaffold front surface is parallel to the velocity at large distances from the disk.
4. The scaffold thickness is small and permeable to fluid flow but we will assume that the velocity of the fluid in the scaffold is small compared with V_∞.
5. The pressure gradient is equal to the pressure difference per unit length along the scaffold, $\Delta P/L$, and is given by the drag force on the scaffold per unit volume as per the text by Happel and Brenner,[24] where the force due to drag on a circular cylinder is given by:

$$F = \frac{4\pi\eta V_\infty R}{\ln(2R/L) - 0.72}, \tag{2}$$

where R and L are the radius and length of the scaffold, respectively.

6. The rate of internal fluid perfusion within scaffolds may then be calculated as follows:

$$V = -\left(\frac{K}{\eta}\right)\frac{\Delta P}{L}, \tag{3}$$

where V is the velocity of the fluid flow through the porous scaffold, K is Darcy's permeability constant.

We note here that a similar mathematical perfusion flow rate has been described elsewhere by our laboratory.[25] In this study, we modified our numerical model to permit the parametric analysis of internal fluid perfusion based on the properties of scaffold geometry. Parametric analysis of fluid perfusion through the scaffold was performed as a function of pore size, pore volume, and pore channel tortuosity. Also, three values of external fluid velocity, V_∞, were considered in the analysis representing a low (10 mm/s), medium (50 mm/s), and high (100 mm/s) rate of scaffold velocity as described by Botchwey et al.[25] We note here that for systems of direct perfusion, fluid flow rate through the scaffold may be measured directly and is not calculated theoretically.

Characterization of nutrient diffusion and flow-induced nutrient flux

To evaluate the role of nutrient diffusion and consumption within cell-seeded scaffolds in the absence of flow, we have developed a 1D glucose diffusion model with the following assumptions:

1. The pores within the scaffold are cylindrical with a uniform distribution of glucose consumption sources, $Q\ g \cdot s^{-1}m^{-1}$, within each of the pores. Q is given by:

$$Q = \frac{N\hat{r}}{nl}, \tag{4}$$

where N is the total number of cells within the scaffold, $\hat{r}$ is the single osteoblast glucose consumption rate, n is the number of cylindrical pores within the scaffold, and l is the length of the modeled pores.

2. In the absence of flow, diffusion within the scaffold is given by[26]:

$$D\sigma\frac{\partial^2}{\partial x^2}C(x) = -Q, \tag{5}$$

where D is the diffusivity of glucose, σ is the average cross-sectional area of the modeled pores, and $C(x)$ is the concentration of glucose as a function of depth within the scaffold.

3. The boundary conditions are given by:

$$C_0 = C(0) \text{ and } \frac{\partial}{\partial x}C(l/2) = 0, \tag{6}$$

C_0 represents media glucose concentration at the exterior boundary of the scaffold. Symmetry of glucose concentration within the pores in the absence of flow results in the 0 value of the derivative. The analytical solution to the boundary value problem is then given by:

$$C(x) = C_0 - \frac{N\hat{r}}{2Dn\sigma l}(Lx - x^2), \tag{7}$$

Glucose diffusion was modeled under typical conditions of microcarrier scaffold culture as reported previously.[19] We have also derived relevant data from a report by Goldstein et al.[17] involving similar high-density bone cell cultivation within 3D scaffolds.

Characterization of flow-induced nutrient flux

Nutrient consumption during dynamic culture was examined by calculating 1D glucose transport flux due to internal fluid perfusion within the scaffold during culture. For all calculations, glucose consumption within the pores was assumed to be homogeneous (i.e., uniform as function of depth along the pore). The volume of fluid medium, ΔM, delivered within the pores of the scaffold is:

$$\Delta M = n\sigma\Delta x, \tag{8}$$

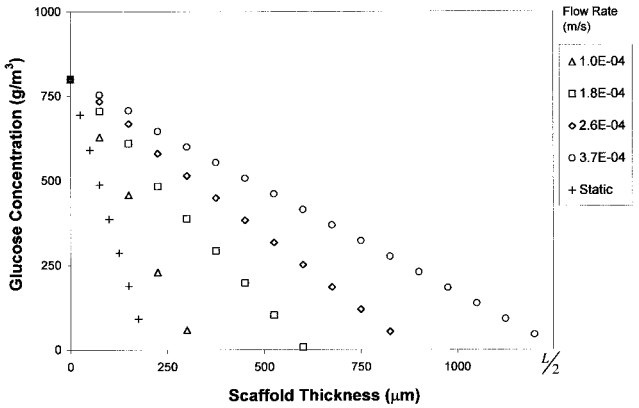

Figure 1. Changes in glucose concentration within microcarrier scaffolds as a function of internal perfusion rate. Parameters for scaffold architecture and cell density were described previously in our laboratories.[19] Modest increases in internal fluid perfusion have profound effect on internal glucose concentration. As shown, a minimal internal perfusion rate of approximately 0.00037 m/s is necessary to maintain positive glucose concentration throughout the construct of thickness $L = 2.5$ mm.

where Δx is the incremental depth within the modeled pore, and where n and σ were defined previously as the number of model pores within the construct and the average cross-sectional area, respectively. The quantity of consumed glucose within this volume, ΔQ, during culture medium perfusion is:

$$\Delta Q = N\frac{\Delta x}{l}\hat{r}T, \tag{9}$$

where T is the average residence time of fluid medium within the volume, and where N is the total number of cells within the scaffold, l is the length scaffold pores, and $\hat{r}$ is the single osteoblast glucose consumption rate as defined previously. Fluid residence time is given by:

$$T = \frac{\Delta x}{V}, \tag{10}$$

where V is modeled internal fluid velocity within the pore. As fluid moves through the pore, the decrease in nutrient concentration, ΔC, within the pore was determined by the following:

$$\Delta C = \frac{N}{n}\frac{\Delta x}{l}\frac{\hat{r}}{\sigma V}, \tag{11}$$

obtained by substituting Equations (8) and (9) into Equation (10). Glucose flux within the scaffolds was calculated for a range of culture parameters in Equation (11) that encompass the experimental conditions previously described[18,19]; however, scaffold cell density was held constant at $N = 1 \times 10^6$. These results are shown in Figures 1 and 2.

To examine the possible differences in dynamic culture systems, we have extended our model for the calculation of internal fluid perfusion and flow-induced glucose flux in spinner flask bioreactors and direct perfusion systems. A schematic representation of three such systems proposed for tissue engineering of bone and their associated methodology is depicted in Figure 3. Internal fluid flow in each systems is achieved in different ways. In spinner flasks, stirred culture medium is moved past the scaffolds at fixed positions within the vessel. In rotating bioreactors, the scaffolds are not fixed, but in continuous free fall within the culture medium during bioreactor rotation. In perfusion cultures, culture medium is directly perfused using a uniform fluid pressure head applied to the scaffolds and fluid. To facilitate the calculation of spinner flask and perfusion culture conditions, characteristic values of exterior fluid flow rates in these systems were taken from the literature and applied to our analytical model of interior flow. For spinner flasks, calculated values of 0.124 and 0.02 m/s were accepted as representative maximum and minimum external fluid velocities as per the text by Gooch et al.[27] For direct perfusion culture, we used a value of 0.03 m/s for internal flow rate as reported by Goldstein et al.[17] Calculated values of internal flow rate were then used to examine the efficiency of these systems to sustain positive glucose concentration as a function of depth within the modeled cell scaffold constructs for reported conditions of dynamic culture.

RESULTS

The results of our numerical modeling of passive glucose diffusion are shown in Figure 4. Based on the geometry and pore architecture of 3D scaffolds studied previously in our laboratory, media glucose is rapidly depleted by cells in the exterior layers of our scaffolds. For comparison, we have also modeled glucose consumption in a similar 3D cell scaffold composite system of larger dimension and overall porosity (Table I). Although glucose penetration depth is larger for such constructs, modeled penetration depth of me-

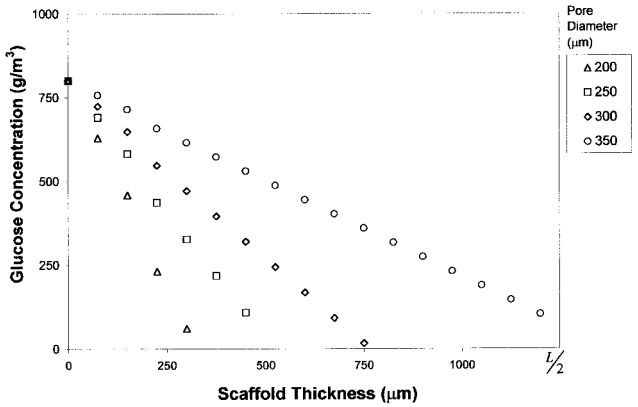

Figure 2. Changes in glucose concentration within microcarrier scaffolds during dynamic culture as a function of scaffold pore diameter. Representative cell density was taken from a previous study,[19] and is listed in Table I. Calculations were performed using an internal perfusion rate of 0.0001 m/s, previously shown to be insufficient to maintain positive glucose concentration throughout the construct (Fig. 5). As shown, increases in pore diameter significantly enhance nutrient flux within microcarrier scaffolds even at minor internal fluid perfusion flow rates.

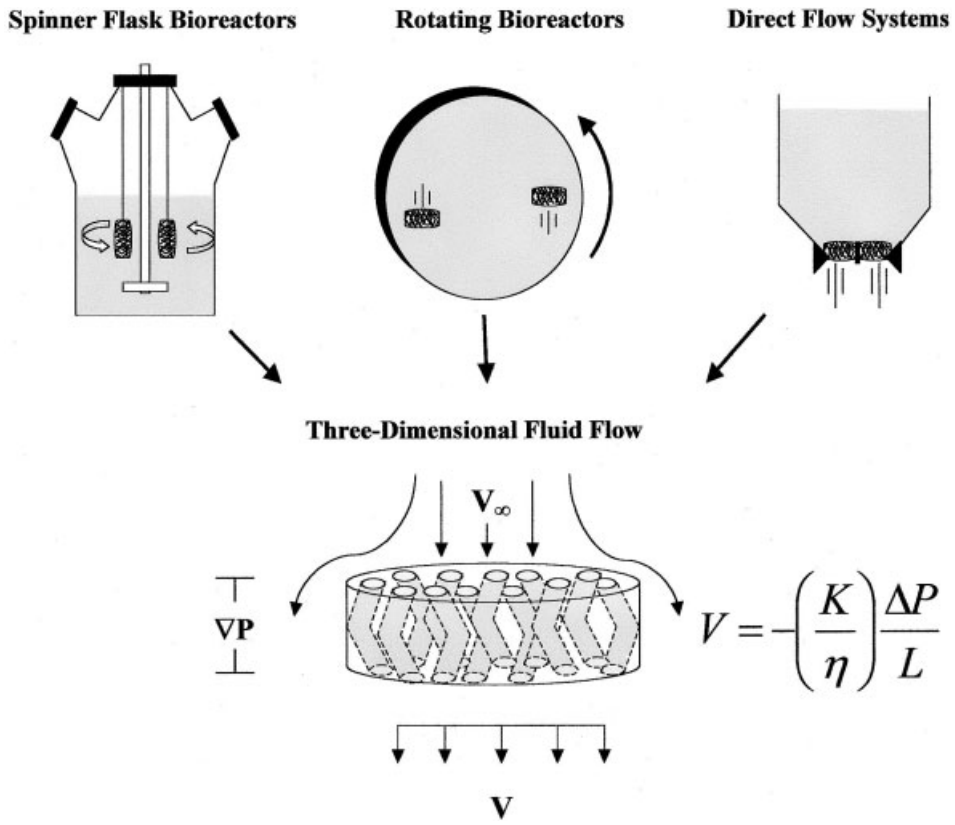

Figure 3. Representative overview of dynamic culture methods used to obtain fluid flow and nutrient flux in porous, 3D scaffolds. In spinner flask bioreactors, culture medium is stirred around scaffolds at fixed positions within the vessel. In rotating bioreactors, scaffolds are maintained in continuous free fall through the culture medium. And finally, in a direct flow system, scaffolds are fixed in position and perfused with culture medium by a direct application of a uniform fluid pressure head. In each case, the flow of fluid on and around the scaffolds leads to a pressure gradient, ΔP, within the construct. The rate, V, of 3D fluid perfusion through the scaffold can be determined by Darcy's law, where η is fluid viscosity and K is Darcy's permeability.

dia glucose relative to the thickness of the scaffold remains low. In must be noted here that only mean values are derived from the literature and are not meant to determine absolute limits on diffusive limitations or tissue ingrowth. However, the analysis can be used to obtain a rudimentary analytical representation of the realities of static 3D tissue engineering in bone, and to illustrate the importance of providing adequate nutrient supply within 3D constructs.

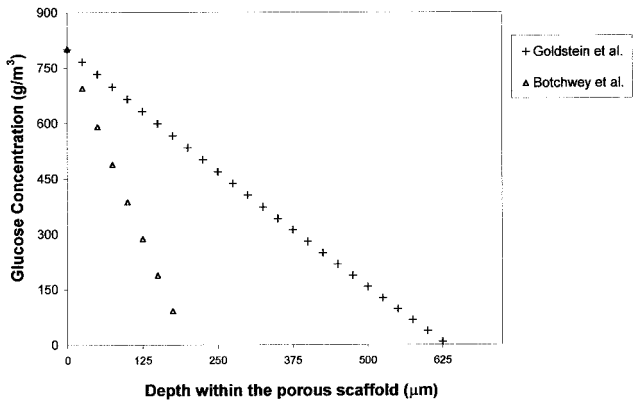

Figure 4. One-dimensional modeling of steady-state glucose concentration as a function of depth within representative 3D cell-scaffold composite systems during static culture. The physical data used for calculations and the references from which they were derived are summarized in Table I.

Figure 5 illustrates a representative composite image of microcarrier scaffold motion in the rotating bioreactor at the near extremes of scaffold velocity. In Figure 5(A), the scaffold is composed entirely of hollow, lighter-than-water microcapsules. The resulting construct has a density of 0.65 g/mL and a velocity through the fluid medium of approximately 100 mm/s. In Figure 5(B), the scaffolds were modified by the inclusion of solid, heavier-than-water beads, and has skeletal density between 0.90 and 0.99 g/mL. In this case, the velocity of scaffold motion is approximately 10 mm/s or less. Using the mixed microcarrier methods described by Botchwey et al.,[25] scaffolds have been produced to span this range of densities and scaffold velocities.

In this study, we have chosen model scaffold velocities of 100, 50, and 10 mm/s to use in the calculation

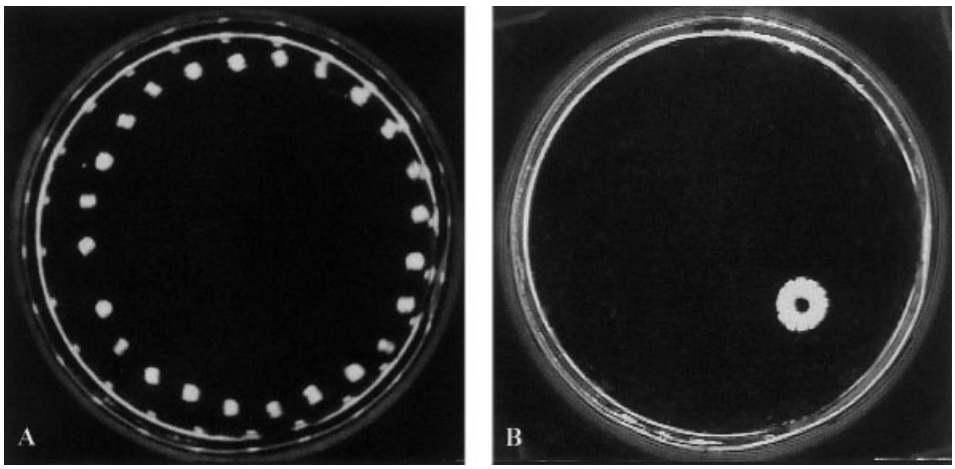

Figure 5. *In situ* imaging analysis of representative scaffold motion in the rotating bioreactor. In the laboratory frame of reference, the bioreactor is rotating in a counter-clockwise direction. The z axis is perpendicular to the plane of the paper. Microcarrier scaffolds adopt a primary circular trajectory in a clockwise direction with instantaneous speed determined from the position (x,y) of the microcarrier and the frame capture rate. Secondary motion is characterized by an inward centrifugal drift from the external vessel wall to center. The images are representative of the extremes in scaffold velocity observed in this system. Scaffolds with approximately 0.90 g/cm^3 density exhibit instantaneous speed through the fluid medium of 10 mm/s (A) and scaffolds with density of 0.70 g/cm^3 have instantaneous speeds of 100 mm/s (B).

of internal fluid perfusion rate and nutrient flux within the scaffolds. Internal fluid perfusion rates are calculated based on these scaffold velocities and a broad range of physical scaffold properties, as shown in Figure 6. Internal flow rate increased linearly with pore volume from a maximum of approximately 0.01–0.001 m/s. In the range of tortuosity ($\tau = 1$–3) describing most porous materials,[24] internal flow rates ranged from 0.008 to 0.002 m/s. Variation in pore diameter in the range required for tissue ingrowth, namely 100–300 μm, produced a range of internal fluid flow rates from 0.002 to 0.011 m/s, respectively.

Under dynamic culture conditions, the contributions of flow-induced transport of glucose are significant. Based on our theoretical model, the maximum depth of modeled glucose penetration increases linearly with internal perfusion rate (Fig. 1). Under the conditions of culture reported previously by our laboratory, and minimal perfusion flow rate of approximately 7.4×10^{-5} m/s is required to deliver glucose throughout the depth of our microcarrier scaffolds. This result is significantly impacted by pore size, where the maximum depth of modeled glucose is directly proportional to the cross-sectional area of the modeled pores (Fig. 2).

Figure 7 further illustrates the importance of dynamic culture conditions and associated levels of perfusion flow for 3D bone cultivation. In this example, three model systems are considered, representing the aforementioned modes of 3D dynamic culture proposed previously for bone tissue engineering. In spinner flask bioreactors, experimental parameters such as impeller size and rate of rotation may be selected to produce a broad range of fluid eddy velocities within the flask. Our data suggest that successful culture in this system is dependent on the selection of appropriate dynamic culture conditions. For perfusion cultures, internal fluid perfusion rates accepted from the literature would be effective in delivering adequate nutrient flux within our microcarrier scaffolds. For rotating bioreactors, the representative minimum and maximum values of modeled scaffold velocity also supply sufficient internal perfusion and nutrient flux within the modeled scaffolds, although the gradient in nutrient concentration is much steeper under minimal flow.

Figure 8 shows representative osteoblast-like cell growth within microcarrier scaffolds cultured for 7 days under static [Fig. 8(A)] and dynamic [Fig. 8(B)] conditions. To visualize interior cell growth, scaffolds have been stained for alkaline phosphatase expression and dissected along the central axis perpendicular to the plane of the cylindrical constructs. Qualitative assessment of osteoblast-like cell growth under static conditions shows preferential growth generally confined to the outer 300–700 μm regions of the construct. This result is in reasonable correlation to theoretical predictions of maximum glucose penetration within the pores of the scaffold. In contrast, cell growth under dynamic 3D conditions is shown throughout the depth of the construct. However, on the exterior regions of the scaffold, limited cell growth occurs on polymer microspheres directly exposed to fluid flow. Figure 9 shows a top view of a dynamically cultured scaffold before coarse sectioning. Under the particular conditions of dynamic culture considered, cells do not

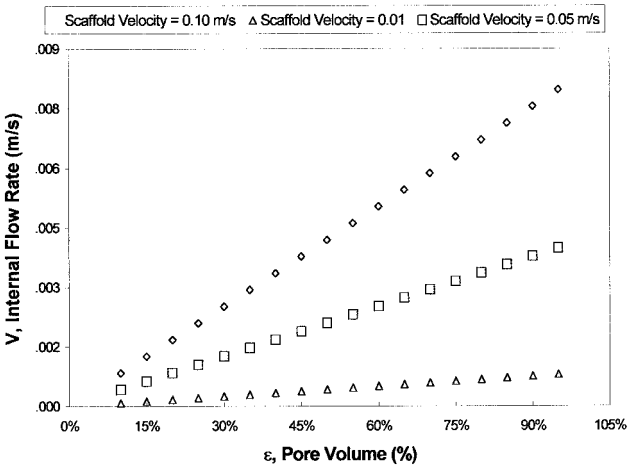

(a)

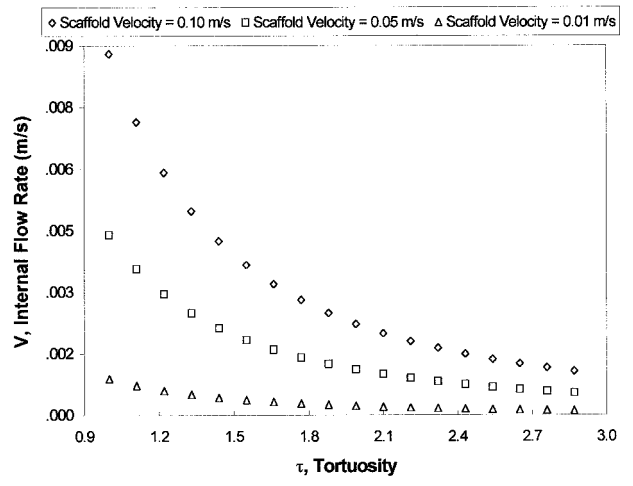

(b)

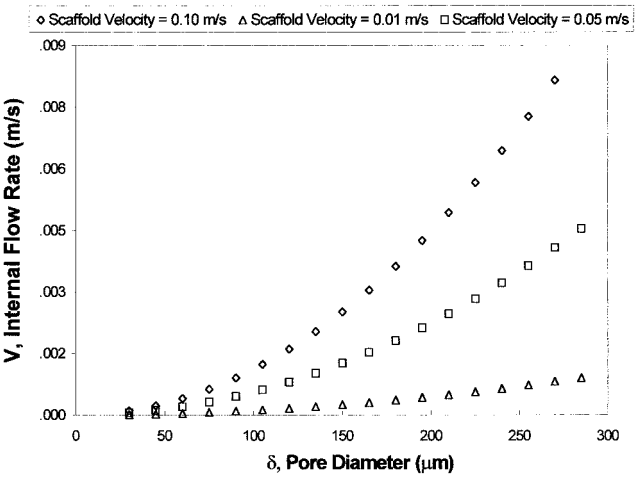

(c)

Figure 6. Parametric analysis of fluid perfusion within 3D scaffolds as determined by theoretical modeling. Internal perfusion rates are calculated based on three representative values of measured scaffold velocity ranging from 0.1 to 0.01 m/s reported previously by Botchwey et al.[18] Scaffold geometry and pore architecture have a profound effect on the rate of interior fluid flow. As shown, internal fluid flow rate increases rapidly with increasing scaffold pore volume (A). Increasing pore channel tortuosity results in significant decreases in flow rate (B). Internal fluid flow rate increases rapidly with increasing scaffold pore diameter (C).

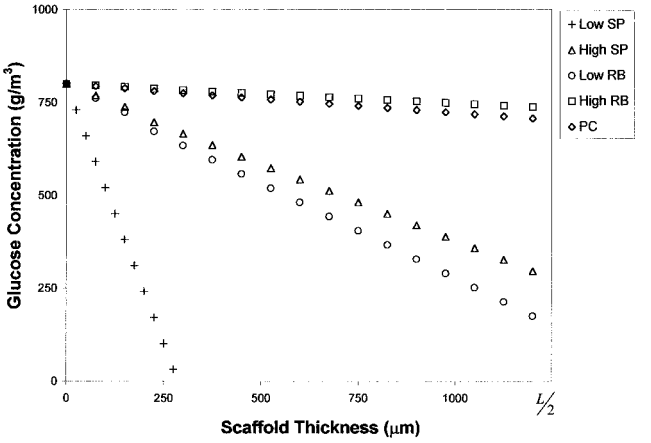

Figure 7. Modeling of glucose concentration as a function of depth within microcarrier scaffolds under representative dynamic culture conditions. Low SP and High SP are defined as the modeled minimum and maximum exterior flow conditions respectively in spinner flask bioreactors as reported by Gooch et al.[27] Low RB and High RB are defined as respective minimum and maximum of exterior flow conditions in the rotating bioreactor as reported previously by our laboratory.[19] PC is given by the perfusion flow conditions reported by Goldstein et al.[17]

fully cover the outer microspheres and limit themselves to regions exposed only to internal fluid flow.

DISCUSSION

Given the strong metabolic demands of osteoblastic cells during mineralized tissue formation, effective nutrient delivery has long been considered an important factor for successful tissue engineering of bone. Considerable qualitative evidence of nutrient diffusive limitations has been reported,[5,6,15–18,28] but few studies have sought to quantify the effects of nutrient diffusion during high density *in vitro* cell cultivation. Therefore, we have developed a 1D model to evaluate glucose diffusion in culture within porous scaffolds in the absence of flow. In the range of modeled scaffold geometry and pore architecture studied, our results showed that passive glucose diffusion was insufficient to maintain minimum glucose concentration beyond a few hundred microns within modeled constructs. These results are not surprising given the *in vivo* result of nutrient limitations and cell hypoxia at distances greater than 200 μm from a blood vessel. In addition, these results are consistent with prior experimental observations of osseous tissue ingrowth within 3D scaffolds proposed for bone tissue engineering.[5,6] Al-

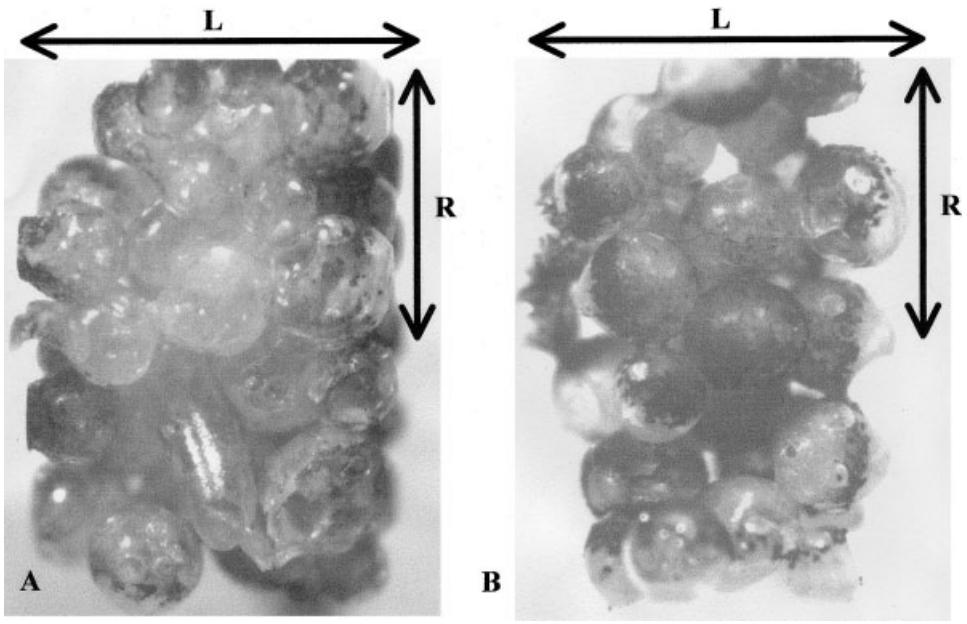

Figure 8. Alkaline phosphatase staining (shown in black) of SaOS-2 human osteoblast-like cells within bisected 3D microcarriers scaffolds after 7 days under static (A) and dynamic (B) culture conditions. Scaffolds' properties and conditions of cell cultivation have been reported by Botchwey et al.[19] Scaffolds were sectioned with a surgical blade to visualize cells on the scaffold interior. Cells stained positively for alkaline phosphatase were clearly visible on the periphery of the scaffold after 7 days of static culture, but no cells were present within the scaffold interior where glucose concentration is insufficient to maintain cell viability (A). In contrast, osteoblast-like cells appear to completely and preferentially cover the microcarriers on the interior of the scaffolds cultured with rotation, and cell ingrowth spans the entire depth of the 2.5-mm structure (B). Black arrows indicate the scaffold thickness, $L = 2.5$ mm, and cylindrical radius, $R = 2$ mm, respectively.

though more rigorous quantitative work remains to be performed, we believe that these studies provide a basis for dynamic tissue engineering of bone to overcome the limitations of passive nutrient diffusion in 3D culture.

In this study, we have combined previously reported methods of *in situ* imaging analysis with a basic mathematical model of fluid flow in porous media in order to quantitatively describe the fluid flow environment within microcarrier scaffolds during culture in the rotating bioreactor. Having demonstrated previously our ability to control scaffold velocity and associated exterior flow in culture between 3 and 100 mm/s,[25] we have examined the effect of scaffold geometry on internal fluid perfusion at three model values of scaffold motion which span the range of these attainable external velocities. Our results show that physical parameters, such as total pore volume, pore diameter, and pore tortuosity of the scaffolds, have a significant effect on internal perfusion and may be modified to obtain a range of internal flow rates. As the relationships governing cell function during tissue engineering in response to chemical and mechanical stimuli continue to be elucidated, this analysis may be used to selectively engineer conditions of 3D dynamic culture to enhance mineralized tissue synthesis.

We have extended our quantitative methods to characterize efficiency of associated nutrient delivery

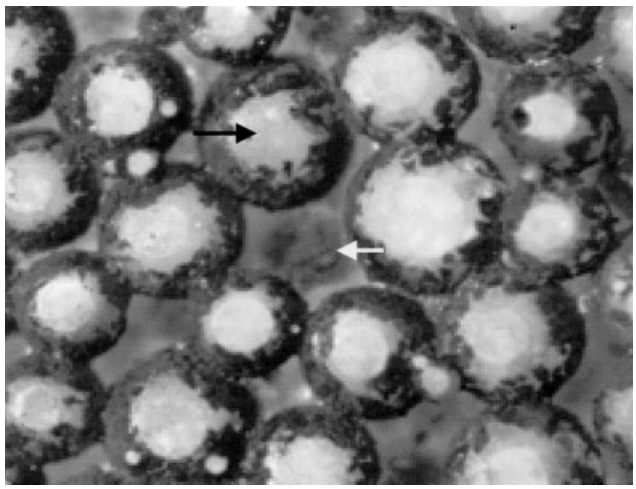

Figure 9. Top view of SaOS-2 human osteoblast-like cell growth on the exterior of microcarrier scaffolds. Cells were visualized by alkaline phosphatase histochemical staining (shown in black) after 7 days of dynamic culture. The direction of culture medium flow around the scaffold during dynamic culture was perpendicular to the plane of the paper. Preferential cell growth was observed in regions exposed only to interior perfusion flow. The black arrow illustrates a noncellular region of a microcarrier on the exterior of the scaffolds surrounded by positively stained osteoblast-like cells on the periphery of the sphere. The white arrow illustrates the surface of an interior microcarrier approximately 600 μm within the scaffold that is covered by positively stained cells.

in our system and other proposed systems based on previously reported dynamic culture conditions. As shown, the ability of these systems to supply necessary nutrient flux throughout modeled microcarrier scaffolds is determined by scaffold design parameters and dynamic culture conditions. Our calculations of nutrient diffusion in the absence of flow indicate that static 3D culture and some inappropriately designed dynamic culture environments lead to regions of insufficient nutrient concentration to maintain cell viability, and can result in steep nutrient concentration gradients within the modeled constructs, the effects of which have not been adequately examined. Some evidence suggests that the concentration of serum agonists such as glucose may be particularly significant to bone cell function under fluid flow conditions.[29–32] For example, Allen et al.[30] showed that Ca^{2+} signaling in bone cells are particularly sensitive to serum supplemented fluid flow in regions of extremely low fluid shear. The results of our model and previously reported estimates of interior fluid shear suggest that such low shear, serum supplemented flow is in fact present in the interior regions of microcarrier scaffolds during cultivation, and therefore, we believe that further study is needed to determine the effects of such environments on cell function during tissue engineering of bone. In the aforementioned studies by Shea et al.,[16] using PLAGA foams in spinner flask culture, it was observed that whereas *in vitro* synthesized tissues near the surface regions of the scaffold resembled native bone, profound changes in tissue architecture were present at increasing depth within the construct. We believe that such observations further underscore the importance of quantifying the conditions of dynamic culture to identify the possible role of nutrition flux within engineered tissues.

Exploratory evaluation of cellular ingrowth within microcarrier scaffolds was conducted by coarse sectioning of the scaffolds after short-term, high cell density cultivation under conditions shown theoretically to provide appropriately balanced levels of glucose interior concentration. Visual evidence of tissue ingrowth suggested that nutrient flux within the constructs was sufficient to maintain viable cells throughout the constructs. These results provide important insight into tissue engineering scaffold design. For example, it may be possible to determine limits to scaffold thickness for a given set of known experimental conditions or physical scaffold parameters, where the parameters are specifically determined by the maximum in nutrient penetration within the construct. However, our results also suggested a need to balance flow-induced nutrient flux with possible deleterious effects of fluid shear stresses. It is possible that fluid shear forces experienced by exterior cells during microcarrier scaffold culture may limit initial cell attachment and growth. In scaffolds engineered for rapid motion during bioreactor cultivation, as shown in Figure 9, cell growth on component spherical microcarriers exposed directly to exterior flow appeared limited in some cases. We believe that such observations may in part be attributed to localized fluid shear forces in these regions. Although prior estimates of exterior stress magnitude in a range from 0.01 to 0.3 N/m^2 should be tolerable to attached cells,[25] to our knowledge, the detachment strength of osteoblast-like cells from PLAGA has not been determined. In addition, the presence of localized turbulent eddies, yet to be quantified within our system, may contribute significantly to localized shear stress.

In conclusion, we have made a basic analytical representation of static glucose diffusion and flow-induced nutrient flux within 3D scaffolds proposed for tissue engineering of bone. Current studies of osteoblast phenotypic expression in three dimensions have not yet fully characterized the *in vitro* tissue morphogenesis of bone. Many factors remain to be quantified such as the transport of oxygen, other nutrients, cell–cell signaling molecules, growth factors, metabolic wastes, and cell chemotactic factors in dynamic culture, all of which may have an effect on cell function and tissue synthesis. Our analytical methods provide an initial basis for quantifying the role of nutrient delivery in 3D culture. More work is needed to quantify the effects of other chemical and mechanical stimuli present in 3D dynamic culture on the physiological development and regulation of *in vitro* synthesized tissues.

C. T. Laurencin was the recipient of the Presidential Faculty Fellow Award from the National Science Foundation. E. A. Botchwey is a Ph.D. fellow of the National Consortium For Graduate Degrees For Minorities In Engineering, and a recipient of the Merck-UNCF postdoctoral fellowship.

References

1. Bone grafts and bone substitutes. Orthop Network News 1999; 10–17.
2. Burwell RG. History of bone grafting and bone substitutes with special reference to osteogenic induction. In: Urist MR, Burwell RG, editors. Bone grafts, derivatives, and substitutes. Oxford: Butterworth-Heinemann; 1994. p 3.
3. Attawia MA, Herbert KM, Laurencin CT. Osteoblast-like cell adherence and migration through 3-dimensional porous polymer matrices. Biochem Biophys Res Commun 1995;213(2):639–644.
4. Attawia MA, Devin JE, Laurencin CT. Development of a 3-dimensional polymer matrix for use in bone repair. Abstracts of Papers of the American Chemical Society. Vol. 208. 1994. p 278-POLY.
5. Ishaug-Riley SL, Crane-Kruger GM, Yaszemski MJ, Mikos AG. Three-dimensional culture of rat calvarial osteoblasts in porous biodegradable polymers. Biomaterials 1998;19(15):1405–1412.
6. Ishaug SL, Crane GM, Miller MJ, Yasko AW, Yaszemski MJ, Mikos AG. Bone formation by three-dimensional stromal os-

teoblast culture in biodegradable polymer scaffolds. J Biomed Mater Res 1997;36(1):17–28.
7. Langer R, Vacanti JP. Tissue engineering. Science 1993;260(5110):920–926.
8. Langer R, Vacanti JP, Vacanti C, Atala A, Freed LE, Vunjak-Novakovic G. Tissue engineering: Biomedical applications. Tissue Eng 1995;1(2):151–161.
9. Laurencin CT, Attawia MA, Elgendy HE, Herbert KM. Tissue engineered bone-regeneration using degradable polymers: The formation of mineralized matrices. Bone 1996;19(1):S93–S99.
10. Laurencin CT, ElAmin SF, Ibim SE, Willoughby DA, Attawia M, Allcock HR, Ambrosio AA. A highly porous 3-dimensional polyphosphazene polymer matrix for skeletal tissue regeneration. J Biomed Mater Res 1996;30(2):133–138.
11. Yaszemski MJ, Payne RG, Hayes WC, Langer R, Mikos AG. Evolution of bone transplantation: Molecular, cellular and tissue strategies to engineer human bone. Biomaterials 1996;17(2): 175–185.
12. Attawia MA, Herbert KM, Uhrich KE, Langer R, Laurencin CT. Proliferation, morphology, and protein expression by osteoblasts cultured on poly(anhydride-co-imides). J Biomed Mater Res 1999;48:322–327.
13. Devin JE, Attawia MA, Laurencin CT. Three-dimensional degradable porous polymer-ceramic matrices for use in bone repair. J Biomater Sci Polym Ed 1996;7(8):661–669.
14. Elghannam A, Ducheyne P, Shapiro IM. Bioactive material template for *in vitro* synthesis of bone. J Biomed Mater Res 1995;29(3):359–370.
15. Ishaug SL, Payne RG, Yaszemski MJ, Aufdemorte TB, Bizios R, Mikos AG. Osteoblast migration on poly(alpha-hydroxy esters). Biotechnol Bioeng 1996;50(4):443–451.
16. Shea LD, Wang D, Franceschi RT, Mooney DJ. Engineered bone development from a pre-osteoblast cell line on three-dimensional scaffolds. Tissue Eng 2000;6(6):605–617.
17. Goldstein AS, Juarez TM, Helmke CD, Gustin MC, Mikos AG. Effect of convection on osteoblastic cell growth and function in biodegradable polymer foam scaffolds. Biomaterials 2001;22(11): 1279–1288.
18. Botchwey EA, Pollack SR, El-Amin E, Levine EM, Tuan RS, Laurencin CT. Human osteoblast-like cells in three-dimensional culture with fluid flow. Biorheology 2003;40(1–3):299–306.
19. Botchwey EA, Pollack SR, Levine EM, Laurencin CT. Bone tissue engineering in a rotating bioreactor using a microcarrier matrix system. J Biomed Mater Res 2001;55(2):242–253.
20. Holy CE, Shoichet MS, Davies JE. Engineering three-dimensional bone tissue *in vitro* using biodegradable scaffolds: Investigating initial cell-seeding density and culture period. J Biomed Mater Res 2000;51:376–382.
21. Borden M, Attawia M, Khan Y, Laurencin CT. Tissue engineered microsphere-based matrices for bone repair: Design and evaluation. Biomaterials 2002;23(2):551–559.
22. Van Belle H. Kinetics and inhibition of alkaline phosphatases from canine tissues. Biochim Biophys Acta 1972;289:158–168.
23. Scheidegger AE. The physics of flow through porous media. 2nd ed. New York: Macmillan; 1960.
24. Happel J, Brenner H. Mechanics of fluid transport processes. 1st ed. The Hague: Martinus Nijhoff Publishers; 1983.
25. Botchwey EA, Pollack SR, Levine EM, Johnston EJ, Laurencin CT. Quantitative analysis of three dimensional fluid flow in a rotating bioreactor. Biorheology 2003;40(1–3):299–306.
26. Petrov N, Pollack SR. Comparative analysis of diffusive and stress induced nutrient transport efficiency in the lacunar-canalicular system of osteons. Biorheology 2003;40(1–3):347–353.
27. Gooch KJ, Kwon JH, Blunk T, Langer R, Freed LE, Vunjak-Novakovic G. Effects of mixing intensity on tissue-engineered cartilage. Biotechnol Bioeng 2001;72(4):402–407.
28. Goldstein AS, Guoming Z, Grayson E, Morris BS, Meszlenyi BS, Mikos AG. Effect of osteoblastic culture conditions on the structure of poly(D,L-lactic-*co*-glycolic acid) foam scaffolds. Tissue Eng 1999;5(5):421–433.
29. Allen FD, Hung CT, Pollack SR, Brighton CT. Serum modulates the intracellular calcium response of primary cultured bone cells to shear flow. J Biomech 2000;33:1585–1591.
30. Allen FD, Hung CT, Pollack SR, Brighton CT. Pertussis toxin inhibits cytosolic calcium increases in osteoblast-like cells stimulated by laminar fluid flow incorporating serum. Trans Orthop Res Soc 1997;22:706.
31. Nollert MU, Diamond SL, McIntire LV. Hydrodynamic shear-stress and mass-transport modulation of endothelial-cell metabolism. Biotechnol Bioeng 1991;38(6):588–602.
32. Shen J, Gimbrone MA, Luscinskas FW, Dewey CF. Regulation of adenine-nucleotide concentration at endothelium fluid interface by viscous shear-flow. Biophys J 1993;64(4):1323–1330.
33. Komarova SV, Ataullakhanov FI, Globus RK. Bioenergetics and mitochondrial transmembrane potential during differentiation of cultured osteoblasts. Am J Physiol Cell Physiol 2000; 279(4):C1220–C1229.
34. Kundu PK. Fluid mechanics. San Diego: Academic Press;1990.